Inhomogeneous Deformation in Welded High Density Polyethylene

Y. Lu, D. M. Shinozaki, S. Herbert

Department of Mechanical and Materials Engineering, University of Western Ontario, London, Ontario N6A 5B9, Canada

Received 29 September 2001; accepted 31 October 2001

ABSTRACT: The effect of the thermal history on the properties of welded high density polyethylene is studied. The lamellar microstructure observed in the weld is different from that in the bulk slow cooled material. The weld has lower crystallinity and smaller lamellar size, both of which change with annealing. The differences in the microstructure between the weld and the surrounding material produce differences in the plastic properties. The low ductility of the welded samples is a direct result of the relatively low yield stress within the weld. Annealing of the weld can improve the tensile properties, but in quenched welds the final properties are still inferior to the bulk material. Displacement controlled, constant velocity microindentation tests are shown to provide a rapid means of evaluating the properties of the weld. © 2002 Wiley Periodicals, Inc. J Appl Polym Sci 86: 43–52, 2002

Key words: lamellar microstructure; welded polyethylene; plastic inhomogeneity; microindentation

INTRODUCTION

In melt welded polymers the thermal history of the material varies from point to point across the weld. In a typical butt welding process, for example, in the joining of a large diameter high density polyethylene (HDPE) pipe, heat is applied to the mating surfaces, the two surfaces are pressed together, and the weld is allowed to solidify by cooling. Barber and Atkinson showed that, depending on the section thickness and the melt temperature, the cooling rates vary over a wide range at different locations in and out of the weld.[1] They examined the gradation in the coarse microstructure in and near the weld using low magnification scanning electron microscopy on chromic acid etched surfaces. The quality of the weld was measured using tensile tests on specimens machined to a uniform cross section gauge length, and the relatively thin weld plane was oriented perpendicular to the tensile axis.[2,3]

The slow crack growth behavior of PE gas pipe was examined by Lu et al.[4–7] Under the conditions used for welding, it was suggested that the cooling rate and molecular orientation in the weld zone influenced the fracture properties. The pressure applied during the welding process affected the flow of residual contaminants out of the molten zone during the welding process.

The present experiments were designed to distinguish between good and bad welds from the practical viewpoint. To this end the relationship between the microstructure and the mechanical properties of a weld in HDPE was examined. It was shown that the weld performance is dependent on the homogeneity of the microstructure and the mechanical properties across the weld.

EXPERIMENTAL

The starting material (pelletized HDPE) was obtained from Dow Chemical. It was a general purpose blow molding resin with a melt flow index of 0.32 g/min. The pellets were compression molded into rectangular bars (6.5 × 5 × 0.2 cm). These were cut to 4 × 1.25 × 0.2 cm and butt welded in an apparatus that allowed the ends of two bars to be melted through contact with a double sided hot plate. The molten ends were then forced together and held until solidification was completed. A variety of melt temperatures were used. After comparing the properties of the welds prepared from different melt temperatures, a melt temperature of 190°C was chosen to study the effect of varying initial microstructures and the effect of post-weld annealing.

Different quenching media (air and water held at different temperatures) were used to change the cooling rate and thus the initial microstructures. Using the slowest and fastest cooling rates, air cooled and brine water quenched (−16°C) samples were annealed for

Correspondence to: D. Shinozaki.
Contract grant sponsor: NSERC.

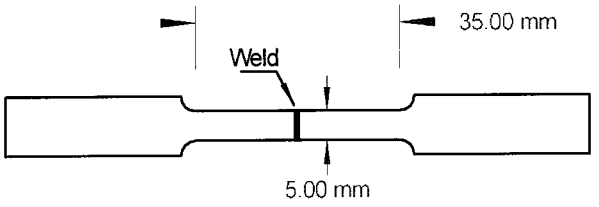

Figure 1 A tensile bar showing the weld plane perpendicular to the tensile axis.

different times at 115°C (below the melting temperature).

Tensile bars were machined from the welded sample with the weld plane oriented perpendicular to the tensile axis (Fig. 1). Similar samples were prepared from unwelded material of the same thickness. Constant displacement rate tensile tests were run at room temperature using two nominal strain rates of (7 and 14) $\times$ 10^{-4}/s, respectively. The tests were run in a standard screw-driven Instron tensile tester at room temperature.

The thermal properties of the weld and bulk materials were measured using a Perkin–Elmer DSC 7 differential scanning calorimetry (DSC) apparatus. Relatively small samples (5 mg) were cut from within the weld zone and from the bulk material. A scanning rate of 20°C/min was used, covering the temperature range of 35°C $< T <$ 160°C. The instrument was recalibrated using two low melting point metals and the baseline was checked on a regular basis to ensure consistency among all tests.

Lamellar microstructures were examined using thin film replicas of permanganic acid etched samples. The etching procedure followed the work of Olley and coworkers[8,9] as reported by Shinozaki and Howe.[10] The two stage replicas were examined in a transmission electron microscope in bright field. Large areas of the specimen were examined at low and high magnification to obtain representative microstructural views. One large specimen was used in studying the variation of the lamellar structure across the weld, and images were taken sequentially from the same specimen across the weld so the subtle variations could be reliably compared between the bulk and the weld.

The local mechanical properties in welded and nonwelded (bulk) material were measured using a microindenter as described previously.[11,12] The instrument consisted of a piezoelectric driver with a flat faced cylindrical microindenter. The diameter (d) of the tip could be changed over a wide range ($15 < d < 300$ μm), but most of the tests in the present experiments used $d = 36$ μm. The tip could be moved in displacement or load control. For deep penetration testing, the tip velocity was set at 5 μm/min, which corresponds to a tensile strain rate of approximately 5 $\times$ 10^{-3}/s.[12] In load control the indentation creep tests were run at a constant applied load of 1 MPa (force/tip area).

RESULTS AND DISCUSSION

Phenomenology of weld deformation

The weld zone was readily distiguishable using transmitted light optical microscopy with crossed polars (Fig. 2). The darker region in the center of the specimen was the weld zone. The overall thickness of the weld plane was approximately 400–600 μm, depending on the weld temperature. This was considerably larger than the microindenter tip diameter used later to characterize the properties within the weld zone. At the lowest melt temperature used (160°C), the weld zone was thinner and a thin central plane of the weld showed different optical contrast, which was a defect arising from the low melt temperature and similar to the central defect. This was the "remnant skin" described by Barber and Atkinson,[2] and it was undoubtedly responsible for the very poor mechanical properties shown below. The overall contrast of the weld showed there was a general molecular orientation within the zone and a different structure within the central thin defect plane for the low temperature weld. This was consistent with the observations reported by Barber and Atkinson.[1]

The tensile properties of the weld bar were measured with the tensile axis perpendicular to the weld plane (Fig. 1). A decreasing weld temperature caused the overall ductility to decrease (Table I), and with the lowest temperature of 160°C (for which the central oriented zone was observed in Fig. 2) the deformation was highly localized within the weld zone [Fig. 3(d)].

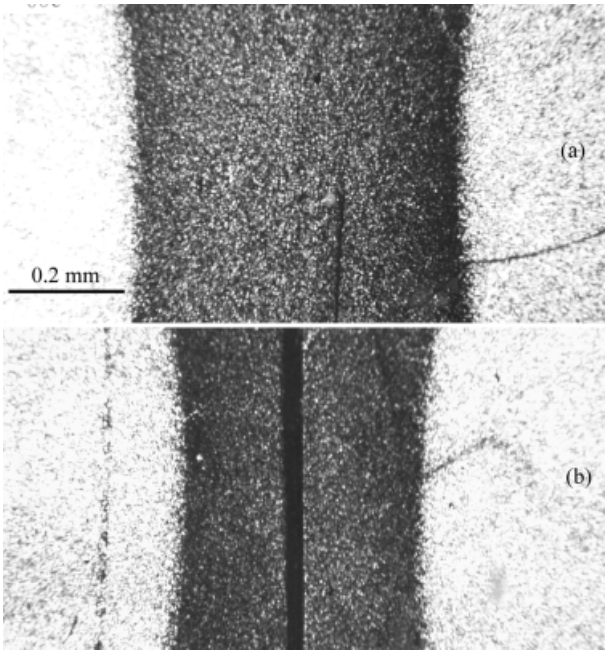

Figure 2 Optical micrographs of welds with weld temperatures of (a) 190 and (b) 160°C. The images were recorded in transmitted light using crossed polars.

TABLE I
Effect of Welding Temperature on Nominal Tensile Properties

		Strain rate = 7×10^{-4} s^{-1}		Strain Rate = 14×10^{-4} s^{-1}	
	Welding temp. (°C)	Yield stress (MPa)	Ductility	Yield stress (MPa)	Ductility
Bulk		31.2	No fracture		
Welding temps.	160	−29.8	0.02	10.2	0.01
	190	30.5	0.04	25.2	0.022
	280	30.1	>0.08	28.1	0.046

The tensile strain rate is the nominal displacement rate/gauge length of the tensile bar.

At higher strain rates the weld showed very low ductility, but for slowly deformed samples the weld showed more plastic flow within the weld itself. At the two lower weld temperatures the plastic deformation is highly localized within the weld proper. Although the highest weld temperature shows general necking and yielding, including the bulk and weld material, the neck shoulder is much sharper and more localized than for the bulk tensile specimen [Fig. 3(a)], which is also indicative of a higher degree of localization of plasticity within the weld.

It was clear that the tensile behavior of the welded bars was strongly affected by the loading rate; and, when reducing the rate, even relatively bad welds (160°C) could appear to have reasonable yield strength and some modicum of ductility (Table I), at least within the weld. However, the overall ductility for the welds was low compared to the bulk unwelded material, which showed the normal necking and drawing process.

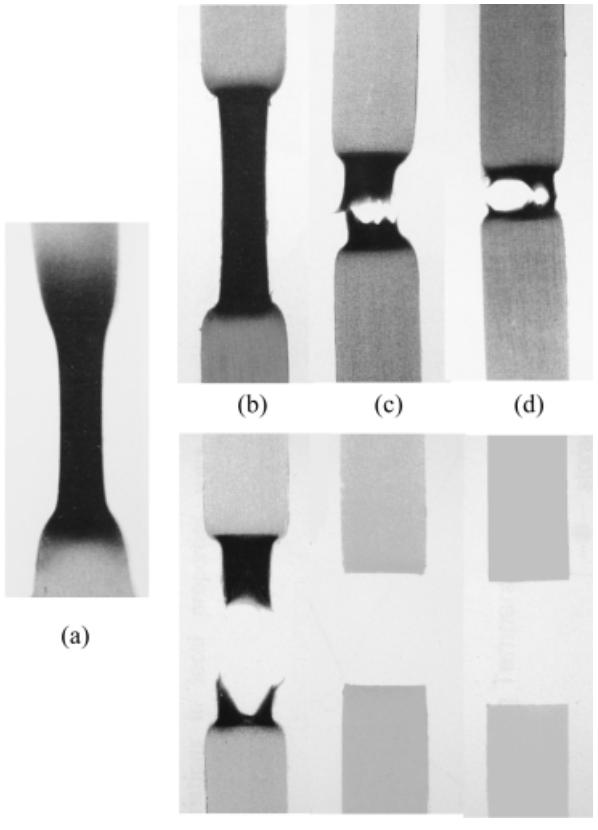

Figure 3 The deformed regions within the tensile bar gauge length for (a) bulk unwelded and different weld temperatures of (b) 280, (c) 190, and (d) 160°C. The top row of specimens was tested at a nominal strain rate of 7×10^{-4}/s and the bottom row of specimens was tested at 14×10^{-4}/s.

For quenched welds the postwelding annealing at 115°C resulted in a progressive increase in ductility and a small increase in yield stress with increasing times at the temperature [Fig. 4(a)]. However, even after 120 min of annealing, the mechanical properties remained markedly inferior to the unwelded bulk material. In contrast, for a slow cooled welded specimen, the annealing process resulted in tensile properties that were similar to the bulk material after the long annealing time [Fig. 5(a)]. For both the quenched and slow cooled welds, the low nominal ductilities measured in the tensile tests were manifested in the specimen as localization of the deformation within the weld [Figs. 4(b), 5(b)]. Only for the slowly cooled fully annealed sample [Fig. 5(b), sample (a)] was extensive cold drawing observed. Thus, the tensile tests, combined with visual examination of the specimen after testing, were useful in distinguishing between good and bad welds.

Microstructural origins of weld strength variations

The mechanical properties of the welded HDPE were dependent on its microstructure, which was completely described only by characterizing the crystalline content, the lamellar thickness, and the arrangement of lamellae. These microstructural parameters were expected to be different in the weld zone and the bulk material. The tensile test of the welded bar involved the loading of the weld in series with the bulk material, so the sample was effectively a series coupled composite.

The low magnification optical micrographs (Fig. 2) showed apparently sound welds result from most welding conditions, except for those in which the welding temperature (the melt temperature) was too low (160°C). Almost all welded bars had tensile properties that were inferior to the slow cooled bulk HDPE, especially at higher loading rates.

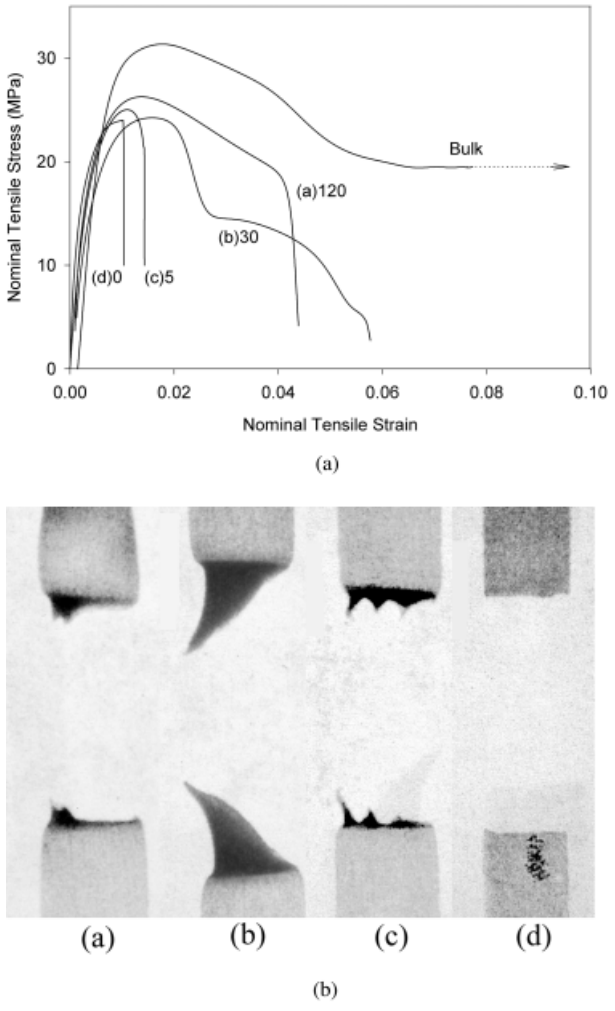

Figure 4 (a) The tensile stress–strain curves for a quenched weld followed by annealing at 115°C for the various times (min). A bulk unwelded sample is shown for comparison. (b) The failure modes of the tensile specimens from (a).

A closer examination of the lamellar structure in and out of a high temperature weld showed that the microstructures were different (Fig. 6). The etched surfaces covered the entire weld, and the lamellar structures showed a smooth transition from one structure to the other and no evidence of microscopic solidification cracks within the weld. At higher magnification, the bulk slow cooled material typically showed a more highly organized lamellar structure (Fig. 7). The effect of even faster cooling could be found in the small weld bead that solidified more rapidly than the weld within the body of the sample (Fig. 8). The structure here showed no evidence of the long-range parallel arrangements of lamellae seen in Figure 7(a). This cooling rate dependence of the lamellar organization was expected, because the long-range regular arrays could only be arranged if given enough time for the molecules to diffuse to the appropriate position.

However, the elimination of gross solidification defects in the welds did not necessarily result in the best mechanical properties for the welded material. The entire thermal history of the weld affected its properties. This is seen in Table II, which shows the tensile ductility varied with the thermal history.

One of the microstructural consequences of variations in the thermal history was that the crystallinity varied widely. The crystallinity within the weld was generally lower than in the bulk slow cooled material. However, cross plots of the tensile ductility of the welded bars and weld crystallinity showed no significant correlation. This was because the nominal tensile ductility (elongation at fracture) was dependent on the plastic constraint in the weld. The influence of the weld crystallinity can be inferred from its effect on the plastic inhomogeneity, which is now explained.

There was generally a correlation between the tensile properties and crystallinity in homogeneous bars (not welded). The yield stress decreased with decreasing crystallinity. An example is shown in Figure 9, in which thin plaques of HDPE were quenched at differ-

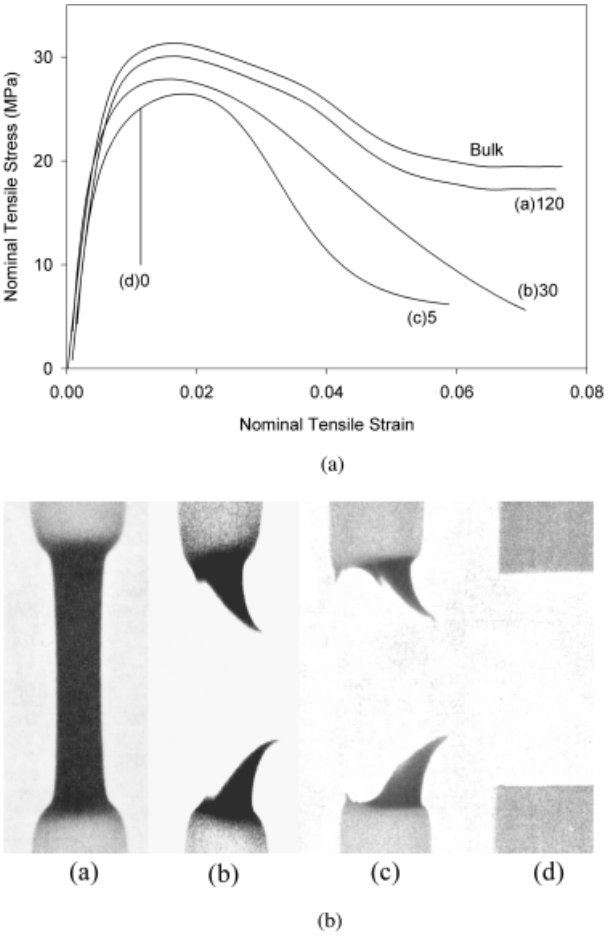

Figure 5 (a) The tensile stress–strain curves for a slow cooled weld, followed by annealing at 115°C for various times (min). A bulk unwelded sample is shown for comparison. (b) The failure modes of the tensile specimens from (a).

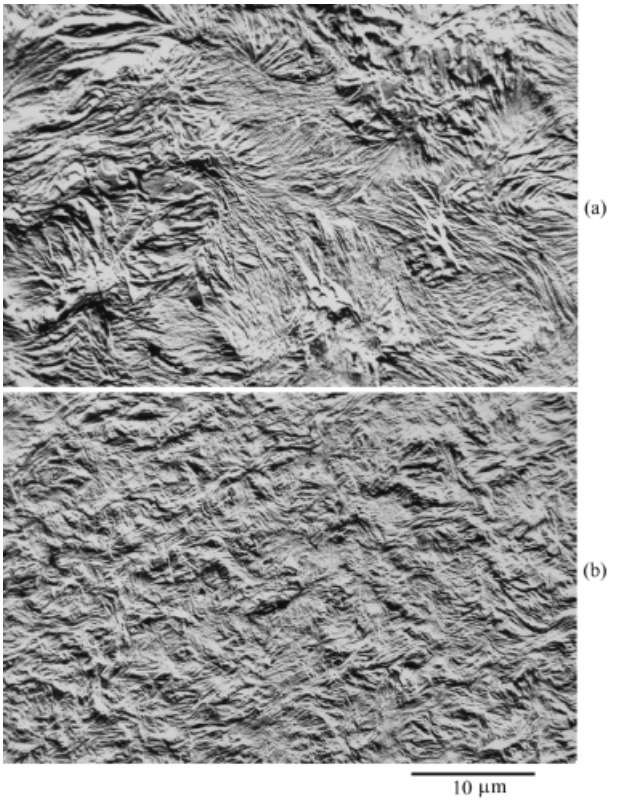

Figure 6 Transmission electron micrographs of replicas of permanganic acid etched surfaces for (a) bulk unwelded and (b) welded samples.

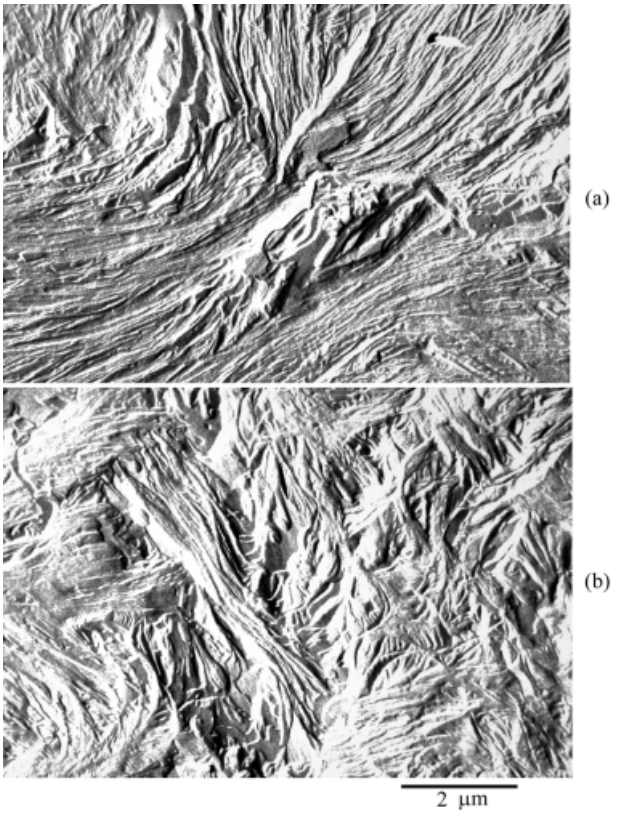

Figure 7 High magnification transmission electron micrographs of replicas of (a) bulk unwelded and (b) welded samples.

ent rates to produce tensile bars with uniform mechanical properties. The crystallinity in these samples was calculated from the area under the crystalline melting endotherm in the DSC scans (assuming a crystalline heat of fusion of 293 J/g according to Wunderlich[13]). The different cooling rates on these plaques spanned a wider range than would have been seen in the weld specimens. The tensile stress–strain curves showed a systematic, reproducible decrease in the yield stress and a decrease in the work hardening rate at strains exceeding the yield strain. The bulk slow cooled sample with a crystallinity of 76% had a nominal tensile yield strength of 31.2 MPa, and the sample with 65% crystallinity had a yield stress of 22 MPa. This latter sample had properties similar to those found for welded material before annealing.

For the tensile bar geometry of Figure 1 the weld was mechanically coupled in series with the bulk slow cooled material, and the tensile stress in each zone was approximately the same. Figure 9 shows that the weld zone material yielded first at Y_b and subsequently plastically deformed along its stress–strain curve. For the thin wide tensile bar, the weld zone deformed to a stress of S_b, at which the bulk material (represented by curve a) yielded ($Y_a = S_b$). The nominal tensile stress–strain curves of Figures 4(a) and 5(a) were in fact the result of series coupled composites in which the phases had the properties represented in Figure 9.

This simple explanation of the localization of plasticity within the softer weld material was complicated by the higher yield strength of the surrounding material. The weld zone was constrained from deforming plastically in the width direction because of the surrounding material that had not yielded. The weld zone therefore deformed in plane strain, resulting in a uniaxial yield stress and a work hardening rate that

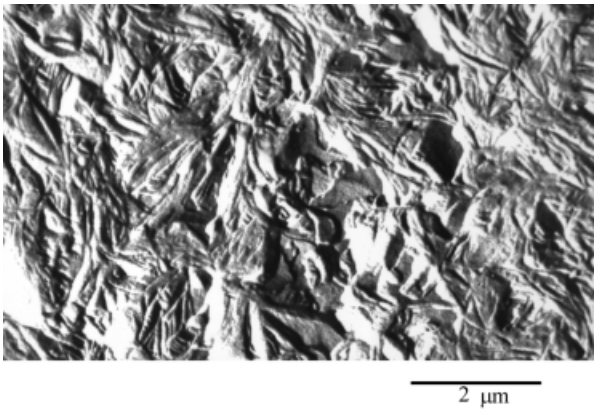

Figure 8 A transmission electron micrograph of a replica for a fast cooled sample taken from the external weld bead.

TABLE II
Nominal Tensile Properties of Welded HDPE

		Tensile yield stress (MPa)	Tensile ductility (nominal strain)
Compression molded slow cooled HDPE (bulk)		31.2	No fracture
Quenched weld	As quenched	24.2	0.01
	Annealed 5 min	25.0	0.02
	Annealed 30 min	25.3	0.057
	Annealed 120 min	27.3	0.044
Air cooled weld	As slow cooled	25.8	0.01
	Annealed 5 min	26.1	0.05
	Annealed 30 min	27.8	0.07
	Annealed 120 min	30.1	No fracture

were higher within the weld than those shown in Figure 9 for the unconstrained material.[14]

The localization of plastic deformation within the weld is seen in Figures 3–5 as darker regions near the failure. The contrast in the images was due to the back lighting of the specimens, which produced increased scattering of the transmitted light in the regions with microcavitation.

A simple conclusion is that the best weld would have a tensile yield stress that is similar to the bulk material surrounding it. The weld is subject to a different thermal history and normally would have a different lower yield stress. The broadly accepted principle of simply reducing the yield stress to improve the fracture resistance does not hold in this case for a welded bar. Failure in welds could thus occur by localization of plastic deformation within the weld and the lack of work hardening capacity to spread the plasticity to the bulk material surrounding the weld.

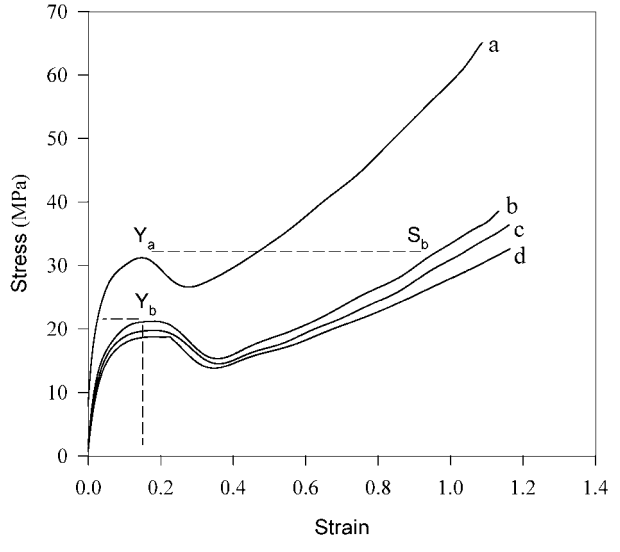

Figure 9 Tensile stress–strain curves for HDPE thin plaques prepared by cooling from the melt at different cooling rates to produce varying crystalline fractions (slow cooled) of (a) 0.76, (b) 0.65, (c) 0.62, (d) 0.58.

The strong constraints within the weld could also generate larger hydrostatic tensile stresses that allow for earlier initiation of microcavitation preceding failure.

Lamellar microstructures

For a melt crystallized weld, the unaided air cooling of the weld results in reduced crystallinity and therefore reduced yield stress [Fig. 5(a)]. Annealing in this case increases the yield stress of the weld zone and, for the reasons discussed above, increases the overall tensile ductility. However, the mechanical properties of the weld are not a single valued function of the crystallinity. Cross plots of the tensile ductility versus crystallinity and the storage modulus versus crystallinity show that it is possible to measure different moduli or ductilities for the same crystallinity. This is expected, because the mechanical properties of a crystalline polymer are strongly affected by its microstructure, which is the arrangement of lamellae, as well as the amount of the crystalline phase. This shows that the distribution of the hard phase (lamellae) is critical in determining the composite modulus and plastic response. In annealing the arrangement of the newly crystallized material is not precisely known, because it constitutes a small fraction of the lamellae (Fig. 6). However, similar studies in other crystalline polymers show that the lamellae that appear with solid-state crystallization are different in arrangement and spacing from those that appear with slow cooling from the melt,[15] and there are resultant differences in the mechanical properties.

In HDPE there are number of studies that show that the lamellar microstructure changes with annealing. The lamellar thickness can be estimated from the melting temperature using the Gibbs–Thomson relationship[13]:

$$T_m = 414.2\left(1 - \frac{0.627}{l}\right) \quad (1)$$

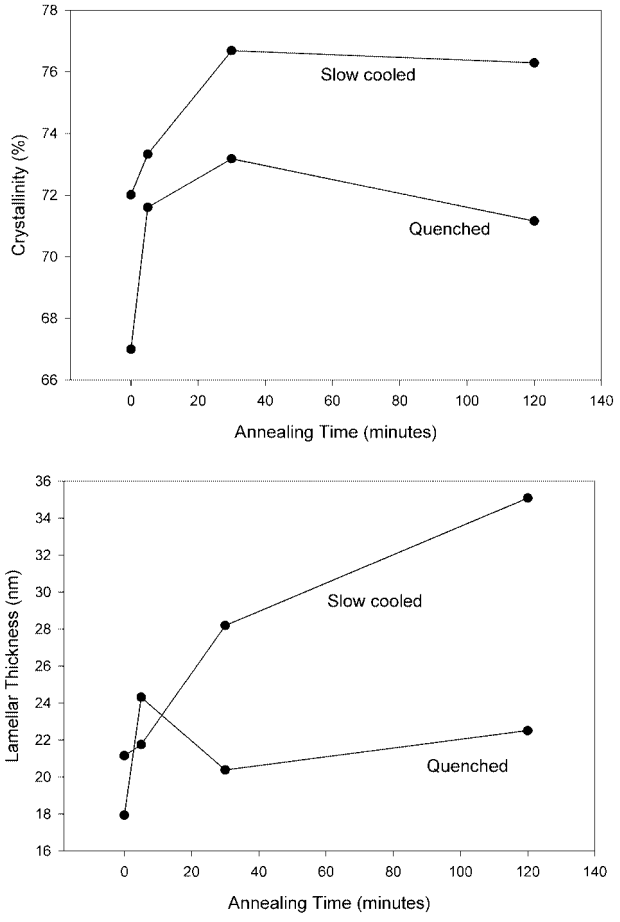

Figure 10 The variation of the crystallinity and lamellar thickness with the annealing time for slow cooled and quenched welds.

where T_m is the melting peak temperature and l is the lamellar thickness (nm). The effect of annealing the weld is shown in Figure 10. The crystallinity and lamellar thickness are both higher in the air cooled sample, as expected. The crystallinity increases in both cases with the increasing annealing time, although the quenched sample does not reach the high crystallinities of the slow cooled samples. Similarly, the lamellar thickness increases for the slow cooled weld but it does not change significantly in the quenched sample.

The simultaneous changes in the lamellar thickness and crystallinity can be clearly seen in Figure 11, in which a thin plaque of HDPE is quenched into liquids of different temperatures. The lower quenching temperatures result in faster cooling, and there are smaller lamellar thicknesses and lower crystallinities. A comparison with the welded bar samples (Fig. 10) shows that the quenched weld (unannealed) has a crystallinity (67%) that would suggest an equivalent quenching temperature of about 118°C in Figure 11. However, the lamellar thickness for the quenched welded bar (18 nm) is similar to that of a plaque cooled into a medium at a much lower temperature. This discrepancy between the crystallinity and lamellar thickness is much less apparent for the slow cooled weld, where the crystallinity indicates an equivalent quenching temperature of about 120°C while the lamellar thickness suggests 100°C.

A possible explanation for this may be found by considering the constraint that develops in the weld region during cooling from the melt. Very rapid quenching results in a large hydrostatic tensile stress field generated by the mismatch in the coefficients of thermal expansion and in the specific volume difference between liquid and crystalline PE. Slower cooling allows the solidification front to move more slowly, allowing for greater relaxation of stresses within the weld zone. There is evidence that lamellar thickening on annealing is pressure dependent.[16] Alternatively, the kinetics for lamellar thickening are generally much slower than for primary crystallization, as observed in long-term annealing experiments with PE.[13]

It might initially be expected in welds that the cooling rate, resulting from the quenched sample, would be less than for the thin plaque; but the lamellar thickness for quenched welds was found to be similar. The material adjacent to the molten zone is approximately at room temperature, provided the heating time was kept small. With intimate contact to the molten zone the initial temperature drop would be rapid. This rapid cooling would be seen only for the first part of the cooling, because the thermal conductivity through the polymer would be poor. Hence, the critical cooling rate over the solidification temperature would be rapid for welds in which the melt temperature is low and in which the two faces are kept in contact with the welding plate for longer times.

In addition, the localized melting of the weld zone, followed by solidification in a planar zone constrained by solid HDPE on either side, would result in residual stresses that slowly decay after welding. The anneal-

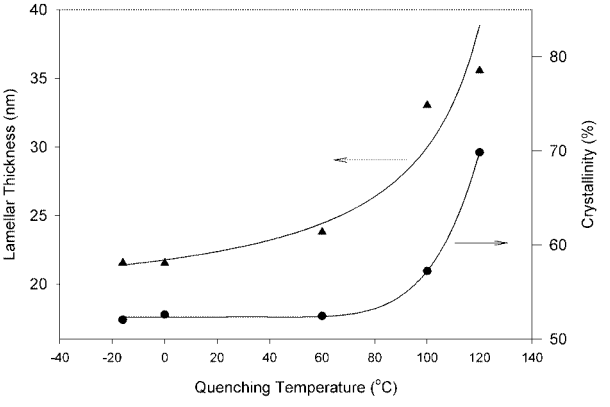

Figure 11 The variation of the lamellar thickness and crystallinity with the quenching temperature from the melt for HDPE plaques. Lower quenching temperatures result in faster cooling rates.

ing process relieves these stresses, although the sample (weld and bulk) should be annealed together to achieve complete stress relief. The recrystallization that occurs during annealing (Fig. 10) initially occurs in the residual stress field and is inevitably influenced by the stress field.

Evaluation of weld quality using microindentation

From a practical viewpoint, the tensile test of the welded bar is a reasonable qualitative test of the weld performance. The ductility and yield stress measure the critical engineering parameters that are of interest in the weld. However, for small welded parts or irregularly shaped components it is not always feasible to prepare a suitable tensile bar with the tensile axis normal to the weld plane. The microindentation test provides a method to test small parts and provides more detailed information about the material properties within the constricted volume of the weld.

Earlier work comparing the dynamic mechanical properties of the weld with those of the bulk HDPE showed that the storage modulus can be used to detect some differences in the mechanical properties of the weld.[11] However, there was no correlation of the storage modulus alone with the nominal ductility or with the yield stress measured using a tensile test of the welded bar. The dynamic mechanical properties were measured at small strains of typically less than 1%. As shown above, the localization of the plasticity and the overall tensile properties were related to the large strain properties of the weld material for which the dynamic mechanical properties were not necessarily a good measure.

The yield strength and work hardening characteristics were related to the microstructure of the weld, which includes the amount of crystalline phase, the lamellar thickness, and the distribution of the phases. The examination of the lamellar microstructure revealed a very complex arrangement of crystalline and amorphous phases for different thermal histories (Figs. 6–8). Direct observation of the microstructure was therefore an insensitive measure of the quality of the weld.

A better indication of the relative strength of the weld could be obtained by comparing the weld yield strength with that of the bulk material surrounding the weld using the deep penetration microindentation test.[12] This test, which uses the same instrumentation as that described for the measurement of the dynamic mechanical properties, was shown to be a rapid and convenient method to measure the local plastic properties. The critical features of the test that distinguished it from standard hardness tests were the flat punch geometry and the constant (controlled) displacement rate of the tip. The constant velocity resulted in a steady-state plastic zone evolving ahead of the moving tip, provided the depth of penetration was greater than about 1 diameter (of the tip). The plastic deformation ahead of the moving flat punch could be modeled analytically and with finite element analysis to reveal the equivalent tensile plastic properties for the polymer. The sample preparation was straightforward, involving the cutting of a sample that included the weld and the bulk material outside the weld. A surface perpendicular to the weld plane was ground flat and polished to an optically smooth finish using metallographic polishing techniques.

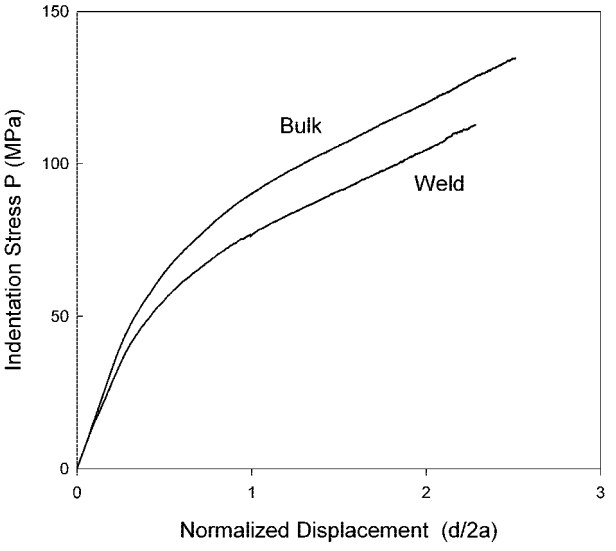

Figure 12 A comparison of the deep penetration stress–displacement curves for the bulk and weld. The diameter of the microindenter was $2a = 36$ μm. The stress is the applied force/area of the indenter face. The indenter velocity was constant.

The microindenter consisted of a flat cylindrical punch with a diameter of 36 μm in this example.[12] Being much smaller than the width of the weld, the penetration load displacement curve was obtained from within the weld zone only or from the bulk only (Fig. 12). Deep penetration curves of this kind were found to be reliably reproducible, and 1 standard deviation (for the "knee" of the curve) was typically less than 3% of the measured value. The tensile yield stress can be obtained from these curves by extrapolating the linear portion of the large displacement region back to zero displacement. The intercept is a measure of the yield stress with the constraint factor defined by Tabor.[17] A detailed analysis showed this simple construction to be accurate for HDPE.[12]

The sensitivity of the deep penetration test in detecting differences in the thermal history of HDPE is shown in Figure 13. Thin plaques of HDPE were quenched to different microstructures over a wide range of crystallinities from 0.58 to 0.76 (a wider range than is normally found in welds, which is 0.67–0.76). The shift in penetration curves to reflect the higher

yield stress is clearly distinguishable, and it was shown to be quatitatively related to the tensile plastic properties.[12]

A more time consuming test to use to evaluate the relative weld properties is the indentation creep test (Fig. 14). Deep penetration analysis shows that the plastic zone ahead of the moving flat punch reaches a steady-state shape.[12] Rather than use the microindenter in displacement control, it was possible to use load control and apply a constant load. The precision of the piezoelectric driver was sufficient to very accurately maintain the loads constant. At constant load the penetration displacement increased slowly with time. The rate of penetration is related to the creep rate in the material being pushed aside in front of the moving tip. Li et al. analyzed the indentation creep behavior of flat indenters in soft materials.[18–20] For the purpose of evaluating weld performance, it was possible to compare the creep performance in and out of the weld. Following the discussion above, the optimization of the weld properties would result in the weld and bulk having the same creep properties, which would imply identical plastic properties.

Microindentation is shown to be useful in characterizing the relative plastic properties of the weld and the bulk. The flat cylindrical tip must be in accurate displacement or load control. In the case of deep penetration displacement controlled testing, the test is rapid and reliable. It can accurately detect differences in the plastic properties of welds. The creep test gives similar information, but it takes much longer to perform. However, it can also be analyzed using Li's methodology to obtain empirical creep properties of the weld. This may be useful in evaluating the performance of the weld under constant loading situations that are common in many applications of welded polymers. Because the specimen size is small, it was shown that it is possible to evaluate the temperature dependence of the weld performance by doing these tests at high temperatures.

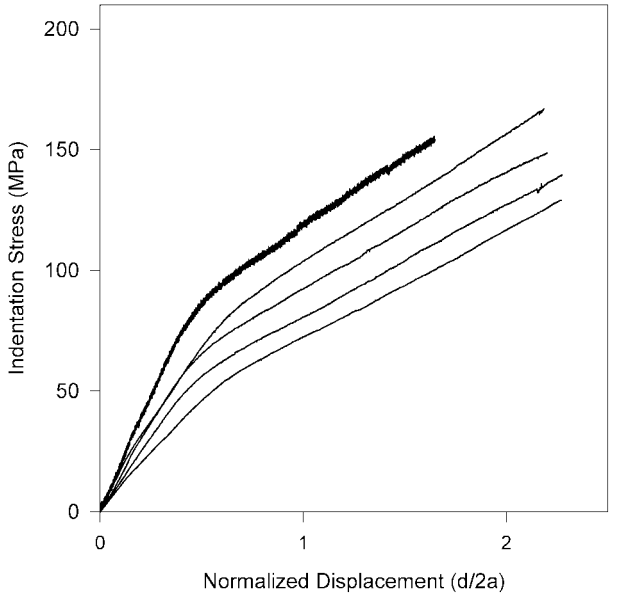

Figure 13 A comparison of the deep penetration stress–displacement curves for HDPE plaques quenched at different rates to produce different crystallinities from a low of 0.58 (softest curve) to a high of 0.76.

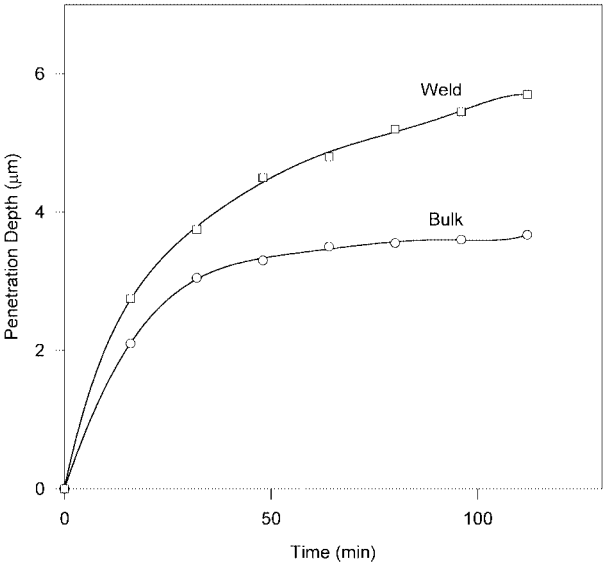

Figure 14 Microindentation creep tests on the bulk and weld. The microindenter diameter was $2a = 0.36$ μm, the applied stress was 1 MPa, and the temperature was 22.5°C.

CONCLUSIONS

The microstructure of melt crystallized welds in HDPE depends on its thermal history, which includes the solidification conditions, and the subsequent annealing. Low melt temperatures and rapid cooling contribute to poor welds that have a low apparent ductility and yield stress in standard tensile tests. The inferior properties of the welded material are related to the inhomogeneity of the plastic properties across the weld. The low yield stress and the work hardening characteristics of the weld that are a complex function of the lamellar microstructure result in localization of plasticity within the weld, which in turn manifests itself as low ductility in the tensile test. Controlled microindentation testing was shown to be useful as a rapid test to accurately characterize the weld quality. Constant displacement rate deep penetration tests were used to straightforwardly measure the local yield stress within the weld. It was found that improved weld properties resulted when the weld yield stress was similar to the yield stress of the bulk material.

The financial support of NSERC is gratefully acknowledged. In addition, much of the work was initiated in discussions with researchers from Dow Chemical (Canada).

References

1. Barber, P.; Atkinson, J. R. J Mater Sci 1972, 7, 1131.
2. Barber, P.; Atkinson, J. R. J Mater Sci 1974, 9, 1456.
3. Atkinson, J. R.; DeCourcy, D. R. Plast Rubber Process Appl 1981, 1, 287.
4. Lu, X.; Qian, R.; Brown, N.; Buczala, G. J Appl Polym Sci 1992, 46, 1417.
5. Lu, X.; Qian, R.; Brown, N. J Mater Sci 1990, 26, 917.
6. Lu, X.; Brown, N. J Mater Sci 1990, 26, 411.
7. Lu, X.; McGhie, A.; Brown, N. J Polym Sci Phys 1993, 31, 767.
8. Olley, R. H.; Bassett, D. C. Polym Commun 1982, 23, 1707.
9. Olley, R. H.; Hodge, A. M.; Bassett, D. C. J Polym Sci Phys 1979, 17, 627.
10. Shinozaki, D. M.; Howe, R. J Mater Sci 1986, 21, 1735.
11. Lu, Y.; Shinozaki, D. M. Polym Eng Sci 1997, 37, 1815.
12. Lu, Y.; Shinozaki, D. M. Mater Sci Eng A 1998, 249, 134.
13. Wunderlich, B. Macromolecular Physics; Academic: New York, 1976; Vol. 2.
14. McClintock, F. A.; Argon, A. S. Mechanical Behavior of Materials; Addison Wesley: London, 1966.
15. St. Lawrence, S.; Shinozaki, D. M. J Mater Sci 1998, 33, 4059.
16. Yasuniwa, M.; Tsubakihara, S.; Yamaguchi, M. J Polym Sci B 1997, 35, 535.
17. Tabor, D. Phil Mag A 1996, 74, 1207.
18. Yu, H. Y.; Li, J. C. M. J Mater Sci 1977, 12, 2214.
19. Chu, S. N. G.; Li, J. C. M. J Appl Phys 1980, 51, 3338.
20. Yang, F.; Li, J. C. M. Mech Mater 1977, 25, 163.